Microfluidic mixing via acoustically driven chaotic advection

Thomas Frommelt, Marcin Kostur, Melanie Wenzel-Schäfer, Peter Talkner, Peter Hänggi, Achim Wixforth

Angaben zur Veröffentlichung / Publication details:

Frommelt, Thomas, Marcin Kostur, Melanie Wenzel-Schäfer, Peter Talkner, Peter Hänggi, and Achim Wixforth. 2008. "Microfluidic mixing via acoustically driven chaotic advection." *Physical Review Letters* 100 (3): 034502. https://doi.org/10.1103/physrevlett.100.034502.

Microfluidic Mixing via Acoustically Driven Chaotic Advection

Thomas Frommelt, Marcin Kostur, Melanie Wenzel-Schäfer, Peter Talkner, Peter Hänggi, and Achim Wixforth

Universität Augsburg, Institut für Physik, Universitätsstrasse 1, D-86135 Augsburg, Germany

(Received 2 August 2007; published 24 January 2008)

Mixing presents a notoriously difficult problem in small amounts of fluids. Herein, surface acoustic waves provide a convenient technique to generate time-dependent flow patterns. These flow patterns can be optimized in such a way that advected particles are mixed most efficiently in the fluid within a short time compared to the time pure diffusion would take. Investigations are presented for the mixing efficiency of a flat cylinder that is driven by two surface acoustic waves. The experimental results favorably agree with model calculations of the flow patterns and the advective transport.

DOI: 10.1103/PhysRevLett.100.034502 PACS numbers: 47.61.Ne, 47.15.G−, 47.52.+j, 47.85.lk

Microfluidic systems have recently attracted remarkable interest, as they represent a promising approach toward the realization of so-called ''labs-on-a-chip'' for biological or chemical applications [1]. Here, the smallest amounts of fluids, containing, for example, biological substances, like cells, are processed and analyzed in minute volumes, far less than a microliter in some cases. There exist various approaches for the different actuation schemes, substrates, and technologies involved. However, due to the physical laws ruling microfluidics, all of these approaches have one thing in common: Efficient mixing, one of the most crucial elements for a fluidic lab-on-a-chip, turns out to pose a severe technological problem. Microfluidics is governed by low Reynolds numbers, measuring the ratio of inertial to viscous forces in a fluid. In a microfluidic system viscous forces are by far the dominant ones, leading to strictly laminar flow. Instabilities and turbulence, being responsible for mixing of macroscopic volumes, are hence ruled out. Even stirring in the low Reynolds number regime does not necessarily imply mixing [2], but only folding of material lines. Thus, diffusion appears to be the only feasible way to achieve mixing in a microfluidic system. On the other hand, especially for large molecules like DNA fragments or oligonukleotides, diffusion is a very slow process, even for small sample volumes. Over two decades ago, Aref *et al.* [3] investigated the passive advection of point particles in a creeping flow agitated by two switchable vortices. Despite the fact that such a flow is laminar for all times, the dynamics of advected particles turns out to be characterized by repeated stretching and folding. This phenomenon, known as ''chaotic advection,'' has attracted considerable attention in theoretical sciences [4].

Experimental mixing approaches strongly depend on the flow geometry. Duct flows have received particular interest recently and many concepts for mixing the channel throughput exist [5]. However, as soon as technologically relevant, arbitrarily shaped, confined volumes like microtiter plate wells or hybridization assays are considered, theoretical and experimental research is missing. Generally, at least one dimension of the volume is too large and cannot be reduced to length scales where diffusion becomes efficient. A combination of low Reynolds and high Péclet numbers quantifying the ration of advective and diffusive transport [6] represents a group of fluidic systems being extremely resistant to mixing. In this fluidic regime, no turbulences occur and the time scales for diffusive mixing of, e.g., DNA in a hybridization assay, are of the order of 10^5 s. Also in terms of experimental and theoretical research, this technologically very important regime has thus far remained nearly unattended [5]. In this Letter, we describe a prototypical microfluidic mixer based on surface acoustic streaming driven by two independently modulated agitation sources. When operating this micro mixer in the regime of *chaotic advection*, we observe a significant enhancement of the mixing efficiency at low Reynolds number $\mathrm{Re} \approx 0.07$ and high Péclet number $\mathrm{Pe} > 4 \times 10^5$ in accordance with a theoretical modeling. This effect is not restricted to a special system geometry.

Microfluidic chaotic mixer.—Our microfluidic mixing experiments are based on the interaction of surface acoustic waves (SAWs) and a fluid on the surface of a planar substrate. SAWs are modes of elastic energy, propagating at the surface of a solid [7]. SAWs can be readily generated on the surface of a piezoelectric crystal by so-called interdigital transducers (IDTs) [8]. These consist of a comblike interdigitated metal structure deposited directly on the substrate surface. Application of a high frequency voltage to the IDT creates a deformation of the surface due to the inverse piezoelectric effect, which excites a SAW. The resonance frequency f of the SAW is given by the IDT layout, finger spacing d, and the substrate acoustic velocity c_{SAW} by $f = c_{\mathrm{SAW}}/2d$. When a SAW with an out-of-plane component of motion encounters a fluid on the substrate surface, it radiates a longitudinal acoustic wave into the fluid. This wave is attenuated on the order of millimeters along the direction of propagation. The wave-fluid interaction in turn induces acoustic streaming [9] within the fluid. The SAW driven acoustic streaming has recently been shown to cause actuation of small liquid droplets

[10] and also to efficiently induce stirring within smallest amounts of fluid, even for very low Reynolds numbers [11].

The flow pattern in a thin layer of fluid agitated by a single IDT located directly under the fluid was investigated in Ref. [2]. There, it was shown that the SAW induced flow velocity is parallel to the layer plane and the advection in such a flow is always laminar. In this single IDT setup, the acoustic streaming is able to induce stirring, but its mixing abilities remain limited. To improve and investigate the mixing performance of a SAW driven microfluidic stirrer, a microflow structure akin to Aref's "batch stirring device" [3] is constructed. We use two IDTs as SAW sources, which generate different flow patterns in a sample if separately operated. The key element of our mixer is the temporal modulation of the two patterns, which can be accomplished by signal modulation of each individual IDT. We show that an "out of phase" power protocol results in chaotic advection, and turns the stirring system into a most efficient mixer.

In Fig. 1, we depict the schematic layout of our planar fluidic chip. In the center, a fluid reservoir is formed between the substrate surface and a glass cover slide. The lateral confinement of the fluid is achieved by chemical modification (silanization with octadecyl trichlore silane, OTS), leaving a hydrophilic area for the fluid surrounded by an otherwise hydrophobic sample surface. A droplet of water on this 1.5 mm diameter hydrophilic spot is vertically confined by a glass slide at a distance of about 240 μm above the substrate surface. The fluid volume ($\approx$0.35 μl) confined between two hydrophilic planes takes the shape of a catenoid, a cylinder with a concave mantel. In order to be able to create different flow patterns on a single chip, special tapered IDTs (TIDTs) [12] have been designed. A TIDT has a nonuniform finger spacing, where the applied high frequency signal generates a narrow

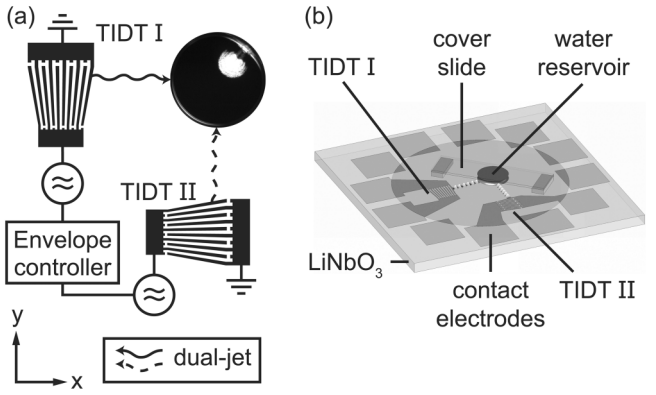

FIG. 1. The SAW mixer chip. (a) Two TIDTs exciting SAWs in x and y directions. An envelope controller runs predefined programs modulating the amplitude of the SAW arbitrarily. The fluid is confined in a catenoidal geometry between the substrate and a glass cover slide. When operating in dual-jet mode, TIDT I works at constant power (solid line), and the power of TIDT II is modulated (dashed line). (b) A 3D view of the SAW mixer chip.

SAW beam only at a specific location on the TIDT, which is given by the local finger spacing fulfilling the resonance condition $f = c_{\mathrm{SAW}}/2d$. Thus, the excitation frequency of each TIDT determines the exact launch position of a narrow SAW beam (width $\approx$ 140 μm), which then enters the fluid volume and causes acoustic streaming. The SAW's entry region, where the fluid is accelerated to high velocities, is further referred to as the "jet." Two TIDTs can be employed to launch SAWs along two normal directions (x, y) of the substrate surface independently (cf. Fig. 1). The piezoelectric substrate in this case is $LiNbO_3$ (128° rot Y cut), providing SAW with out-of-plane displacement for both directions. A low frequency (<10 Hz) power modulation of the TIDT can be applied to cause a temporal modulation of the force acting on the fluid.

We conducted the mixing experiments in three different modi of operation. Here, we present the "dual-jet" setup (cf. Figure 1) while the remaining configurations are available online [13]. In the dual-jet mode, two spatially separated jets are generated by TIDT I at constant power and TIDT II at oscillating power.

To visualize the resulting streaming patterns, a small volume of fluorescent IDC polystyrene latex beads (7×10^{-4} vol%, $\varnothing = 1.5 \pm 0.037$ μm) was injected under the cover slide using a Hamilton 0.5 μl syringe (indicated by the bright spot in the lower left quadrant in Fig. 1). The fluorescence of the beads and the progress of the experiment was monitored using a HUND fluorescence microscope with a video camera attached. To enhance optical contrast, the bottom of the fluidic reservoir was metalized by a thin gold layer. The size of the beads results in very low diffusion constants ($D \approx 3 \times 10^{-13}$ m^2/s) such that diffusion effects can be neglected during our experiments. To ensure reproducibility, all the compared experiments were performed on the very same sample and at a constant temperature ($T = 12\,^{\circ}$C). For this purpose, the chip was mounted on a Peltier cooled sample holder. It underwent a thorough cleaning procedure before it was loaded for subsequent experiments.

Figure 2 displays a series of images taken in dual-jet experiments. The power of TIDT I was held constant during each experiment, whereas the power of TIDT II was modulated at a frequency ν. For better visualization, we inverted the original images; thus, black spots represent bright fluorescent beads. All images of Fig. 2 were taken at $t = 105.6$ s after the experiment had started. Hence, they represent snapshots of the mixing progress. As can be seen already in these static images, the modulation frequency of the oscillating body force represents an important parameter for the mixing efficiency. A more detailed analysis of the experiments presented here resulted in an optimum modulation frequency $\nu = 0.17$ Hz for our experimental dual-jet setup. For modulation frequencies $\nu < 0.17$ Hz [cf. Fig. 2(a)–2(c)], as well as $\nu > 0.17$ Hz [cf. Fig. 2(e) and 2(f)], the mixing is imperfect. One still observes unmixed stripes of high and low bead concentrations.

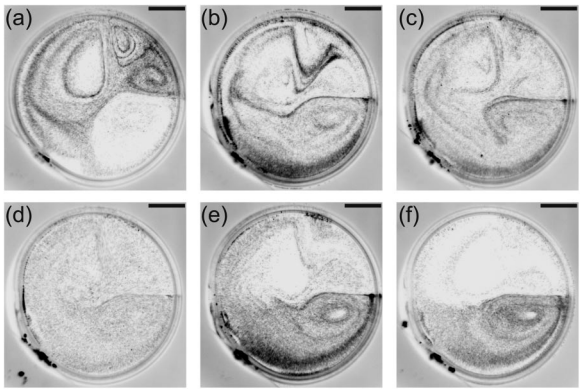

FIG. 2. Top view of the mixing status of dual-jet experiments after $t = 105.6$ s. TIDT I operates at constant power, while the power of TIDT II is constant in (a), and modulated at frequencies $\nu = 0.042$, 0.083, 0.17, 0.34, and 0.68 Hz for panels (b), (c), (d), (e), and (f), respectively. Only for panel (d) at $\nu = 0.17$ Hz, a homogeneous bead distribution is observed (images inverted for printing, scale bar 300 μm).

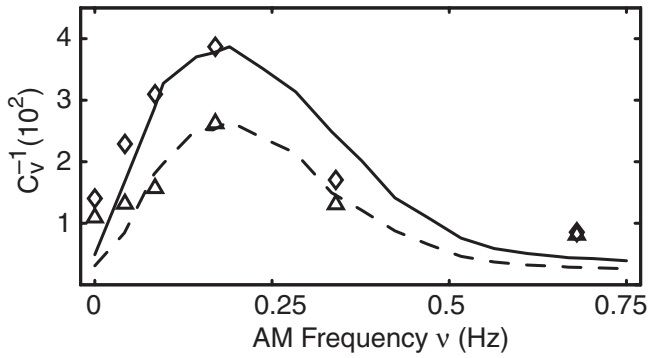

FIG. 3. Quantitative measure of the mixing efficiency c_V^{-1}. For the dual-jet mode, c_V^{-1} is evaluated in the experiment ($\diamond$ $t = 136.0$ s; $\triangle$ $t = 105.6$ s) together with the theoretical result (solid line $t = 136.0$ s, dashed line $t = 105.6$ s) as described in the text. In each case the theoretical curve was scaled to have the same maximal value as the experimental one. The experimental data were taken at two different times after starting the experiment. Optimum mixing is achieved for a modulation frequency of $\nu = 0.17$ Hz for this particular geometry. This optimum frequency is well reproduced in our theoretical description.

Only for the optimal frequency $\nu = 0.17$ Hz the beads exhibit a uniform distribution within the reservoir [cf. Fig. 2(d)] and movie material [13].

In order to quantitatively characterize the mixing efficiency, we processed frame by frame the fluorescence images of a movie [13] taken during the experiments. To avoid edge effects, a circle of 1.12 mm diameter around the center of the reservoir was taken into account. Each frame was divided into square boxes of side length s, and the average gray scale $g_i(s)$ in each ith box was calculated. This gray scale average $g_i(s)$ is a measure for the number of fluorescent tracer particles contained in the ith box. Histograms of gray scales were compiled; for details see Ref. [13]. Deviations from the ideally mixed state can be characterized by the standard deviation of the gray scale distribution $\sigma_{g(s)}$. The inverse coefficient of variation $c_V^{-1} = \overline{g(s)}/\sigma_{g(s)}$ is a well-suited dimensionless quantity representing the mixing completeness on the scale given by the box size s [13]. We chose $s = 74$ μm. Then each box still contains a large number of beads and is small enough to spatially resolve the mixing state of the system [14].

The result of this analysis is presented in Fig. 3 depicting the inverse coefficient of variation c_V^{-1} as a function of the modulation frequency ν for two different times after the initiation of the acoustically induced mixing. An optimum mixing efficiency is observed at $\nu = 0.17$ Hz.

Numerical modeling.—In the numerical modeling of our mixing experiments, we describe the motion of the polystyrene latex beads as the advection of noninteracting point particles. In this way, we neglect effects resulting from the inertia of the particles that in the present situation are extremely small [15]. Moreover, due to their small size and high dilution, any hydrodynamic interactions can safely be disregarded [6]. On the experimentally relevant time scale of a few minutes thermal fluctuations need not be considered because of the small diffusion constant. Under these conditions the particles follow the material lines of the fluid velocity field $\mathbf{v}(\mathbf{x}, t)$ and thus are determined by the following equation of motion $\dot{\mathbf{x}}(t) = \mathbf{v}(\mathbf{x}(t), t)$, where $\mathbf{x}$ denotes the position and $\dot{\mathbf{x}}$ the velocity of a latex bead. The time-dependent velocity field $\mathbf{v}(\mathbf{x}, t)$ results from the SAW generated acoustic wave by means of the acoustic streaming. At the experimentally relevant Reynolds number Re ≈ 0.07, the flow field is described by the Stokes equation of an incompressible fluid driven by an effective body force $\mathbf{f}(\mathbf{x}, t)$

$$\rho \frac{\partial \mathbf{v}}{\partial t} = -\nabla p + \mu \Delta \mathbf{v} + \mathbf{f}, \qquad \nabla \cdot \mathbf{v} = 0, \qquad (1)$$

where p denotes the pressure, ρ the density and μ the shear viscosity of water [6]. The fluid domain assumes a form as in the experiment with rotational symmetry about the vertical z axes and a concave lateral mantel the shape of which is determined by the equilibrium configuration of the force free fluid. Deformations due to the fluid motion are neglected. The fluid is supposed to stick at the substrate and the planar cover, and to obey ideal slip boundary conditions at the free mantel surface.

Each of the two IDTs used in the experiments is characterized by a respective contribution $\mathbf{f}_i(\mathbf{x})$, $i = 1, 2$, to the total force. For the sake of simplicity, they are assumed to be constant with respect to z, and to possess a vanishing z component. The forces rapidly decrease from the points where the acoustic waves enter the fluid. An approximate analytical form of the forces $\mathbf{f}_i(x)$ is detailed in Ref. [13]. In the presence of both IDTs the total body force is a linear superposition of the individual contributions $\mathbf{f}(\mathbf{x}, t) = f_1(t)\mathbf{f}_1(\mathbf{x}) + f_2(t)\mathbf{f}_2(\mathbf{x})$ where the time-dependent coefficients $f_i(t)$ are determined by the mode of operation:

For the dual-jet mode $f_1(t) = 1$ and $f_2(t) = -0.5\cos(2\pi\nu t) + 0.5$. For all time-dependent modes the applied frequencies $\nu < 1$ Hz are slow compared to the relaxation rates of the fluid, which are larger than $\nu_r \approx 6.6$ Hz. Therefore, the relaxation of the fluid velocity toward its asymptotic pattern is considerably faster than the change of the body force such that the time derivative of the velocity field in the Stokes Eq. (1) can be safely neglected. Because of the linearity of the Stokes equation the time-dependent velocity patterns of a particular mode result as the superpositions of the respective patterns generated by the single IDTs, i.e., $\mathbf{v}(\mathbf{x}, t) = f_1(t)\mathbf{v}_1(\mathbf{x}) + f_2(t)\mathbf{v}_2(\mathbf{x})$ where the velocity fields $\mathbf{v}_i(\mathbf{x})$ are the solutions of the stationary Stokes equations with the respective forces $\mathbf{f}_i(\mathbf{x})$ and the boundary conditions specified above. The absolute magnitudes of the force fields acting in the experiments are not known. Therefore, for all setups the velocity was calibrated by the experimentally determined maximum value under a static SAW impinging the droplet. Because the body forces are perpendicular to the z direction and constant with respect to z the resulting streaming patterns are stratified in layers parallel to the substrate. The velocity assumes maximal values in the central plane at $z = h/2$. The advective particle motion is then also restricted to the plane defined by the initial position. Trajectories of 10^4 particles were numerically determined for different initial conditions sampled from a uniform distribution in a spherical region with center at $x = y = -258$ μm and a radius of 194 μm. For a favorable qualitative comparison of theory and experiment we refer the reader to the online material [13].

In order to quantify the mixing performance the coefficient of variation of the number of particles in boxes with side lengths 74 μm covering the fluid volume were determined. In Fig. 3, the inverse coefficient of number variations resulting from the theory are compared to the experimentally determined inverse coefficient of gray scale variation in the dual-jet mode for 2 times $t = 105.6$ s and $t = 136$ s. The theoretical results nicely reproduce the bell-shaped behavior of the experimental inverse coefficient of variation as a function of the frequency ν, displaying a maximum at $\nu \approx 0.17$ Hz in agreement with experiment.

Summary.—The proposed method to mix substances in small amounts of fluids at small Reynolds numbers relies on the effect of chaotic advection and utilizes periodically varying streaming patterns that are acoustically induced by SAWs. We demonstrated the feasibility of this technique in two different modes of operation in experiment and theory. For both modes optimal frequencies characterizing the relevant stretching-folding duty cycles causing the chaotic advection were identified in experimentally accessible frequency regimes.

Based on acoustically driven streaming patterns this mixing technique is extremely flexible: It can be applied to fluids confined in closed channels as well as in open geometries which can be imposed on chips by hydrophilic modification of the substrate. These chips can be produced by planar lithography. Within the regime of validity of the time-independent Stokes equation the mixing speed can be enlarged by increasing both, the fluid velocity (via a larger SAW amplitude), and the driving frequency by the same factor. Combined with other tasks like transport, chemical reactions, and separation of substances the proposed mixing technique may constitute an integral building block of future labs-on-a-chip.

Very useful discussions with Michael Schindler, Christoph Strobl, and Matthias F. Schneider, as well as experimental help from the latter two colleagues and from the members of the Advalytix AG, are gratefully acknowledged. This work was supported by the Deutsche Forschungsgemeinschaft DFG under contracts Nos. SPP 1164 and SFB 486 project B13, and by the German government through the Cluster of Excellence "NIM." The authors thank A. Spoerhase, S. Lieber, and A. Hupfer for their technical assistance.

[1] T. M. Squires and S. R. Quake, Rev. Mod. Phys. **77**, 977 (2005); P. Yager *et al.*, Nature (London) **442**, 412 (2006).
[2] Z. Guttenberg *et al.*, Phys. Rev. E **70**, 056311 (2004).
[3] H. Aref, J. Fluid Mech. **143**, 1 (1984); H. Aref and S. Balachandar, Phys. Fluids **29**, 3515 (1986).
[4] S. Wiggins and J. M. Ottino, Phil. Trans. R. Soc. A **362**, 937 (2004); J. Fowler, H. Moon, and C. J. Kim, *IEEE Conference MEMS, Las Vegas, NV, 2002* p. 97; T. Benzekri *et al.*, Phys. Rev. Lett. **96**, 124503 (2006); H. Zhao and H. H. Bau, Phys. Rev. E **75**, 066217 (2007).
[5] Z. Wu and N. T. Nguyen, J. Micromech. Microeng. **15**, R1 (2005).
[6] J. K. G. Dhont, *An Introduction to Dynamics of Colloids* (Elsevier, Amsterdam, 1996).
[7] G. W. Farnell, *Types and Properties of Surface Waves, in: Topics in Applied Physics*, edited by A. A. Oliner (Springer, Berlin, 1978), Vol. 24.
[8] R. M. White and F. W. Voltmer, Appl. Phys. Lett. **7**, 314 (1965).
[9] W. L. M. Nyborg, *Acoustic streaming, in: Physical Acoustics Vol. II B.*, edited by W. P. Mason (Academic Press, New York, 1965).
[10] A. Wixforth *et al.*, Anal. Bioanal. Chem. **379**, 982 (2004).
[11] K. Sritharan *et al.*, Appl. Phys. Lett. **88**, 054102 (2006).
[12] M. Streibl *et al.*, Appl. Phys. Lett. **75**, 4139 (1999).
[13] See EPAPS Document No. E-PRLTAO-100-082802 for the experimental methods for the generation of the dual-jet flow patterns and other possible operation modes. For more information on EPAPS, see http://www.aip.org/pubservs/epaps.html.
[14] G. Mathew, I. Mezić, and L. Petzold, Physica (Amsterdam) **211D**, 23 (2005).
[15] E. M. Purcell, Am. J. Phys. **45**, 3 (1977).